

This article was downloaded by:

On: 15 January 2011

Access details: *Access Details: Free Access*

Publisher *Taylor & Francis*

Informa Ltd Registered in England and Wales Registered Number: 1072954 Registered office: Mortimer House, 37-41 Mortimer Street, London W1T 3JH, UK



Comments on Inorganic Chemistry

Publication details, including instructions for authors and subscription information:

<http://www.informaworld.com/smpp/title~content=t713455155>

DIRECTIONAL SUPERPARAMAGNETISM AND PHOTOLUMINESCENCE IN CLUSTERS OF MAGNETITE AND CADMIUM SELENIDE NANOPARTICLES

Frank E. Osterloh^a

^a Department of Chemistry, University of California, Davis, CA, USA

To cite this Article Osterloh, Frank E.(2006) 'DIRECTIONAL SUPERPARAMAGNETISM AND PHOTOLUMINESCENCE IN CLUSTERS OF MAGNETITE AND CADMIUM SELENIDE NANOPARTICLES', *Comments on Inorganic Chemistry*, 27: 1, 41 – 59

To link to this Article: DOI: 10.1080/02603590500538654

URL: <http://dx.doi.org/10.1080/02603590500538654>

PLEASE SCROLL DOWN FOR ARTICLE

Full terms and conditions of use: <http://www.informaworld.com/terms-and-conditions-of-access.pdf>

This article may be used for research, teaching and private study purposes. Any substantial or systematic reproduction, re-distribution, re-selling, loan or sub-licensing, systematic supply or distribution in any form to anyone is expressly forbidden.

The publisher does not give any warranty express or implied or make any representation that the contents will be complete or accurate or up to date. The accuracy of any instructions, formulae and drug doses should be independently verified with primary sources. The publisher shall not be liable for any loss, actions, claims, proceedings, demand or costs or damages whatsoever or howsoever caused arising directly or indirectly in connection with or arising out of the use of this material.

DIRECTIONAL SUPERPARAMAGNETISM AND PHOTOLUMINESCENCE IN CLUSTERS OF MAGNETITE AND CADMIUM SELENIDE NANOPARTICLES

FRANK E. OSTERLOH

Department of Chemistry, University of California,
Davis, CA, USA

ZnO microcrystals, $\text{Ca}_2\text{Nb}_3\text{O}_{10}$ nanoplates, and LiMo_3Se_3 nanowires were used to chemically assemble CdSe and magnetite nanoparticles into discrete nanostructures. The CdSe-containing clusters exhibit directional and polarized light emission properties, which are modulated by the one- and two-dimensional morphology of the clusters. Clusters of Fe_3O_4 nanoparticles are superparamagnetic and contain one or two hard magnetic axes, depending on the cluster shape. The ability to control the physical properties of nanoparticles via assembly is of academic and practical interest. Nanostructures with directional emissive and magnetic properties could find applications in light emitting devices, as optical probes, and as magnetic sensors and actuators.

Keywords: nanoparticle cluster, luminescence, superparamagnetism, bottom-up approach

INTRODUCTION

As intermediates between the molecular and the solid state inorganic nanoparticles combine chemical accessibility in solution with physical properties of the bulk phase. This makes them ideal elements for the construction of nanostructured materials with adjustable physical and

Address correspondence to Frank E. Osterloh, Department of Chemistry, University of California, 1 Shields Avenue, Davis, CA 95616, USA. E-mail: fosterloh@ucdavis.edu

chemical properties. Such materials have been realized as films,^[1–5] or as bulk solids.^[6–9] These contain the nanoparticles linked by covalent interactions,^[3–5,8,10] electrostatically,^[2,11–16] via van der Waals interactions,^[1,6,9] or via other interaction types.^[17–22] The physical properties of such assemblies are often quite different from those of the individual nanoparticles, because of dipolar coupling and energy exchange interactions among the closely neighbored components.^[23–25] The hope to exploit such interactions for adjusting the properties of the ensemble or to create entirely new physical properties not present in the separate components are two of the motivations for creating multicomponent nanostructures.^[1,6]

Using suitable synthetic protocols it is also possible to direct the assembly towards discrete nanoparticle clusters (NPCs).^[26–38] Such NPCs contain only a finite numbers of particles and their sizes are on the order of nano- to micrometers. As such, NPCs have the advantage that they can be dispersed in solvents and in matrixes, where they can be used as spectroscopic^[39] or chemical^[30] probes, as catalysts,^[40] or for other advanced applications.^[36,37]

In this paper we review our recent efforts on the construction of NPCs from superparamagnetic and luminescent nanoparticles.^[28,31–34] As we will show here, the physical properties of such structures are dis-


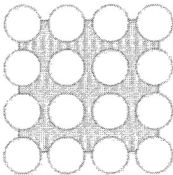
Structure type	Nanoparticle property	
	superparamagnet	semiconductor
1D 	1D Magnetic Anisotropy <i>Nanocompass</i>	1D Optical Anisotropy <i>1D light emitter</i>
2D 	2D Magnetic Anisotropy <i>Magnetic micromirror</i>	2D Optical Anisotropy <i>2D light emitter</i>

Figure 1. Structure-property relationships in nanoparticle clusters.

tinctly influenced and modulated by the cluster geometries (Figure 1). Rod-shaped NPCs have uniaxial magnetic and light emission characteristics whereas plate-like NPCs have two-dimensional anisotropic optical and magnetic properties. Our findings indicate that the anisotropic magnetic properties of these clusters arise from the combination of dipolar interactions among the nanoparticles with their anisotropic three-dimensional distributions. The directional light emission characteristics, on the other hand, seem to be mostly a consequence of the waveguiding properties of the NPC-medium interfaces. The ability of generating directional physical characteristics with nanoparticles via assembly into superstructures is of relevance for engineering properties on the nanoscale. Applications of these structures as microlasers, optical probes, magnetic sensors and actuators, drug delivery vehicles, and display components can be envisioned.

In the following sections we will describe our synthetic approach to these NPCs and describe their structural and physical characteristics, beginning with superparamagnetic structures.

1. SUPERPARAMAGNETIC NANOPARTICLE CLUSTERS

One of the motivations for synthesizing superparamagnetic clusters is to use them as magnetic handles that can be magnetically moved or rotated on the nanoscale. Such superparamagnetic handles could be used as magnetic actuators,^[41] as steering components in magnetically guided self-propelled devices,^[42] as components in spatial light modulators,^[43,44] or as microscale valves in microfluidic systems.^[45] Studies of such structures can also lead to new insight into magnetism on the nanoscale.

Rod-shaped (1D) and plate-shaped (2D) clusters of magnetite (Fe_3O_4) nanoparticles were synthesized according to Figure 2A from nanowires and nanosheets after chemical modification with organic linkers to allow binding of the Fe_3O_4 nanoparticles. For rod-shaped NPCs, LiMo_3Se_3 nanowires^[46,47] were reacted with 3-iodopropionic acid to produce carboxylic acid terminated nanowires. Mixing of the nanowires with an excess of 5.3 nm oleic acid protected magnetite nanoparticles^[48] in THF produced a nanoparticle-nanowire composite. This composite could then be broken into the desired $\text{LiMo}_3\text{Se}_3 \cdot \text{Fe}_3\text{O}_4$ clusters (1) by ultrasonication in THF.

Plate-shaped NPCs (2) were synthesized using exfoliated $\text{Ca}_2\text{Nb}_3\text{O}_{10}$ nanoplates as a 2D template (Figure 2B).^[31,49] Chemical functionalization of the nanoplates with 3-aminopropyltriethoxysilanes produces nanoplates coated with a monolayer of 3-aminopropyl groups. After

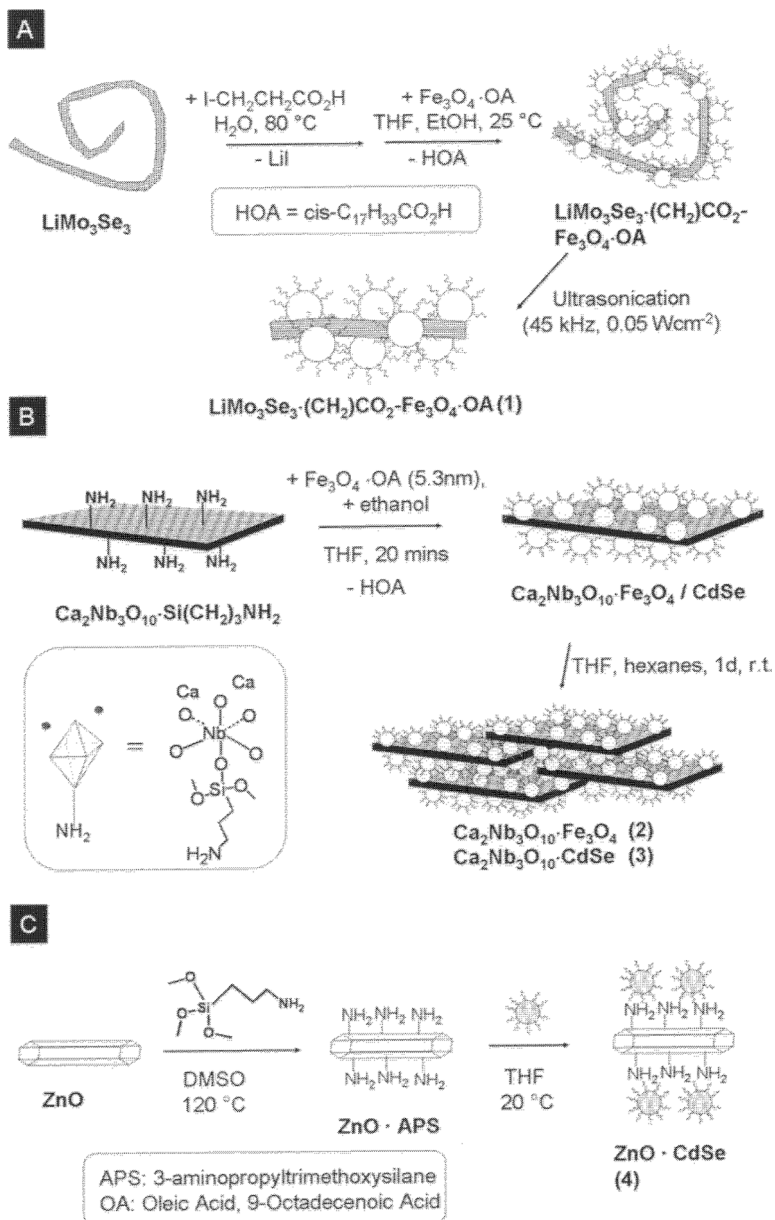


Figure 2. Template strategy for the synthesis of nanoparticle clusters with 1D and 2D morphologies. Reprinted in part with permission from Refs. 31–34. Copyright 2005 American Chemical Society.

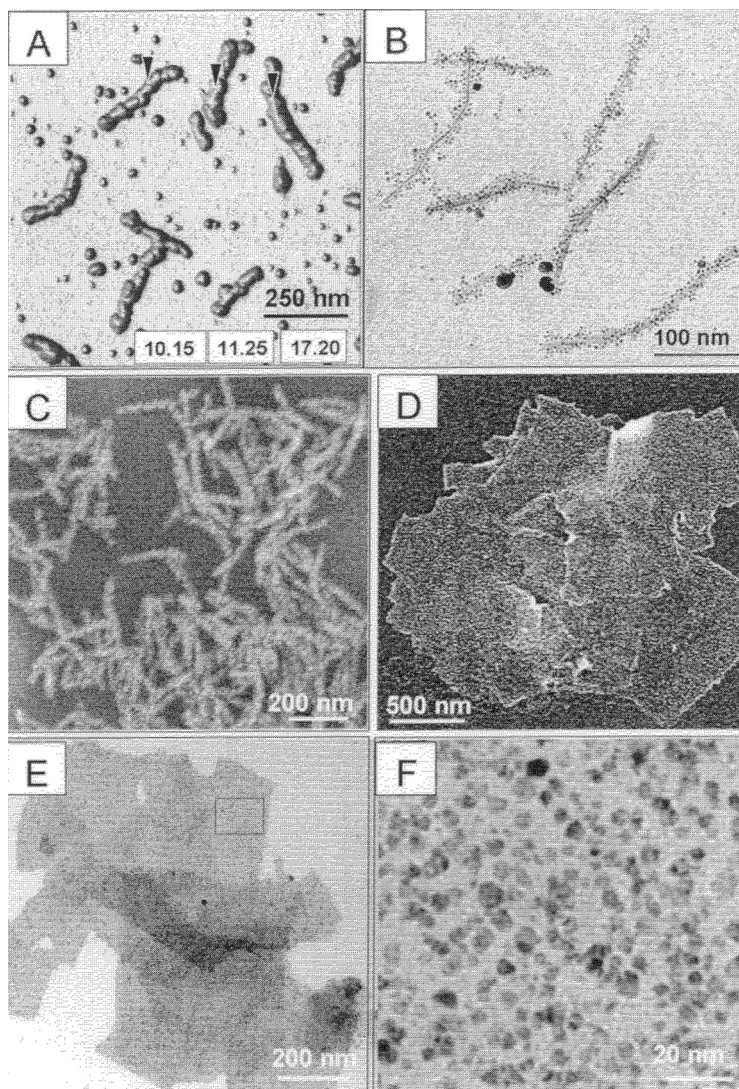


Figure 3. Micrographs of superparamagnetic NPCs. $\text{LiMo}_3\text{Se}_3\text{-Fe}_3\text{O}_4$ (1): A) AFM, B) TEM, C) SEM. $\text{Ca}_2\text{Nb}_3\text{O}_{10}\text{-Fe}_3\text{O}_4$ (2): D) SEM, E) TEM, F) magnified view of rectangular section in E. Reprinted in part with permission from Refs. 31 and 33. Copyright 2005 American Chemical Society.

labeling with an amine-reactive dye, optical spectroscopy of the nanoplates revealed that 21% of the exposed Nb-OH groups on the plates were functionalized with aminopropylsilyl groups. Reaction of the modified plates with an excess of magnetite nanoparticles led to individual $\text{Ca}_2\text{Nb}_3\text{O}_{10}\cdot\text{Fe}_3\text{O}_4$ clusters, which aggregated into clusters (2) *via* stacking in non-coordinating solvents.

According to scanning and transmission electron microscopy, (Fig. 3D–F) rod- and plate-shaped clusters 1 and 2 contain high densities of magnetite particles. In the case of 1, magnetite particles are located on the periphery of 340 nm long and 5 nm wide nanowire fragments. In the case of 2, the nanoparticles are located on either individual plates ($0.16\ \mu\text{m}^2 \times 21.3\ \text{nm}$) or in stacks thereof ($1.6 \pm 0.7\ \mu\text{m} \times 79 \pm 30\ \text{nm}$). For individual plates, $9.3 \pm 0.5 \times 10^3\ \text{Fe}_3\text{O}_4$ particles are located in each $1.0\ \mu\text{m}^2$ on each side of the plate. The average surface-to-surface distance of Fe_3O_4 nanocrystals on these plates is $1.6 \pm 0.5\ \text{nm}$.

Magnetic measurements reveal that NPCs 1 and 2 differ from the isolated nanoparticles in regard to their blocking temperatures (100 K for rod-like 1 and 150 K for plate-like 2), which are increased compared to those found for the free nanoparticles (30 K). The difference between the two blocking temperatures indicates dipolar interactions between magnetic nanoparticles in the clusters, which stabilize the magnetic moments of the Fe_3O_4 nanoparticles against thermal fluctuations.

Because the dipolar interactions have a non-symmetrical distribution (caused by the 1D or 2D nanoparticle distributions) a shape-dependent superparamagnetism of the clusters arises. For the plate-like NPCs two easy magnetization axes along the plates and one hard magnetization axis perpendicular to the plates are experimentally confirmed on films of aligned clusters (Figure 4A). The magnetic anisotropy manifests in different hysteresis loops for a parallel and perpendicular orientation of the NPCs with regard to the external magnetic field, i.e. the planar clusters are easier to magnetize in the plate directions than perpendicular to it. Also, at 5 K, the remanence of the plates in parallel direction is by a factor of 2.3 larger than in the perpendicular directions. Calculations for the two orientations of 2 show that the magnetic field created by the ensemble of magnetic particles stabilizes the orientation of in-plane-dipoles and destabilizes out-of-plane dipoles (Figure 4B). For the NPC rods (1), similar interactions lead to an “easy” magnetic axis along the principle geometrical axis of the rods and to two “hard” axes perpendicular to the rod axis.

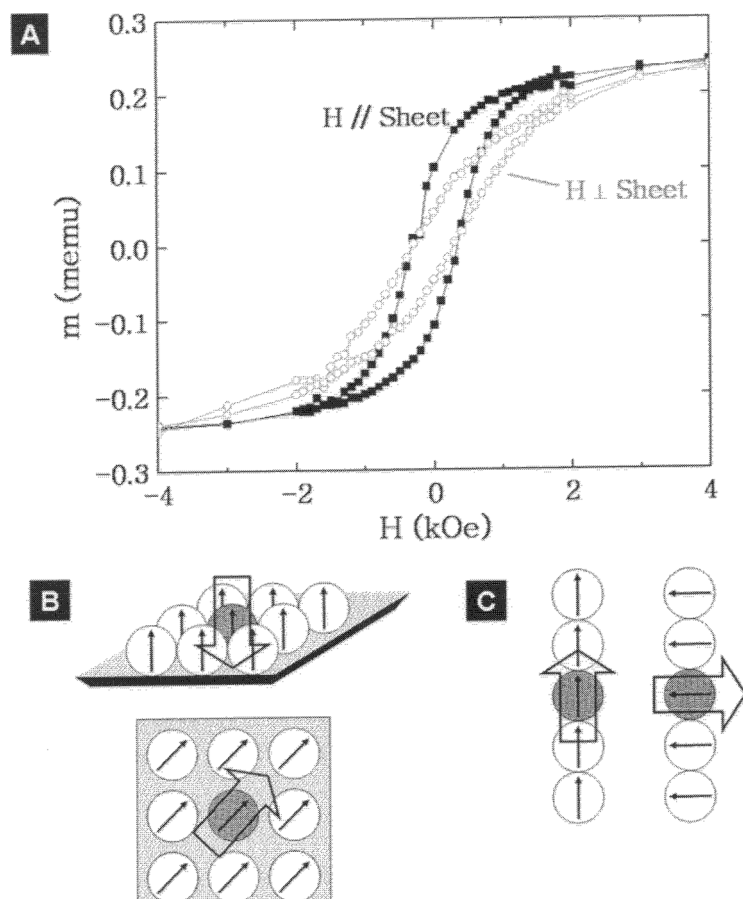


Figure 4. A) Hysteresis curves (5K) for two orientations of 2 with regard to the applied field. B) Schematic depictions of the intrinsic magnetic field generated by the collection of Fe_3O_4 nanoparticles. For rod-shaped 1 the intrinsic field (hollow arrow) stabilizes the magnetic moments of the nanoparticles in the direction of the longer rod axis and it destabilizes them perpendicular to the rod axis. Analogous orientations of the intrinsic fields are shown for plate-shaped clusters. Out of plane moments are destabilized and in-plane moments are stabilized by the intrinsic magnetic field. Reprinted in part with permission from Ref. 31. Copyright 2005 American Chemical Society.

Due to their magnetic anisotropy it is possible to align rod-shaped and plate shaped NPCs with a weak magnetic field. Rod-shaped NPCs (1) deposited from THF solution onto a silicon wafer in a 200 Oe magnetic field show a characteristic alignment along the magnetic field lines

(Figure 5AB). This alignment takes place within about 30s (the time it takes the solvent to evaporate). Because of their larger sizes, the magnetic orientation of plate-like clusters (2) can be monitored in real-time. Figure 5C shows a group of colloidal plates (6.8×5.4 and $2.8 \times 3.2 \mu\text{m}^2$) freely dispersed in THF, under the influence of a 500 Oe inhomogeneous magnetic field (a movie in mpeg format is available in the Supporting Information for reference^[31]). In the first row of the figure, the plates are rotated around an in-plane axis and in the second row of the figure the particles are rotated around an out-of-plane axis. An analysis of the video-microscopy images reveals that the magnetic plates align one of their two in-plane-magnetic “easy” axes with the magnetic field, while

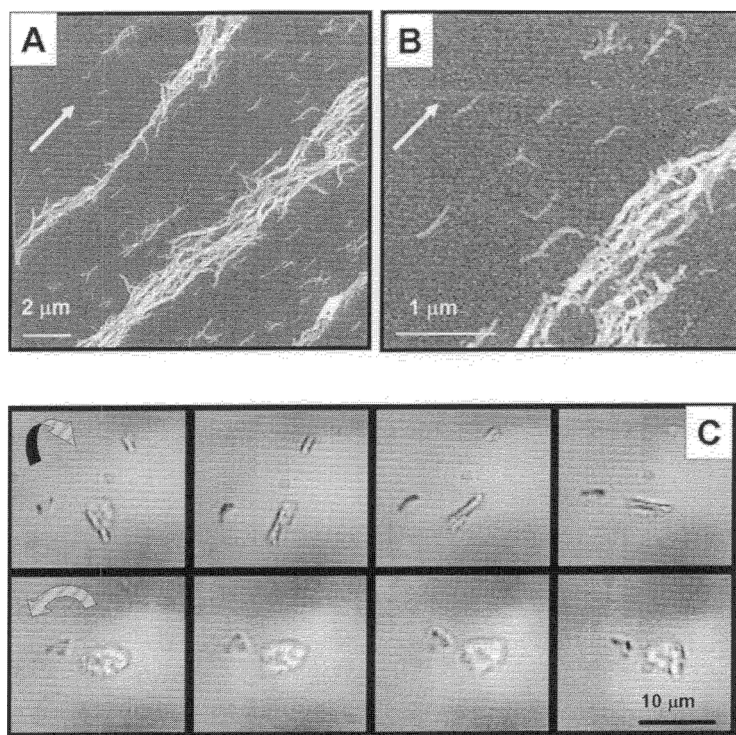


Figure 5. Scanning electron and optical micrographs showing the magnetic orientation of rod- (A, B, magnified view) and plate shaped (C) superparamagnetic NPCs. Arrows indicate the direction of the magnetic field lines (A, B) or the direction or rotation (C). Reprinted with permission from refs. 31 and 33. Copyright 2005 American Chemical Society.

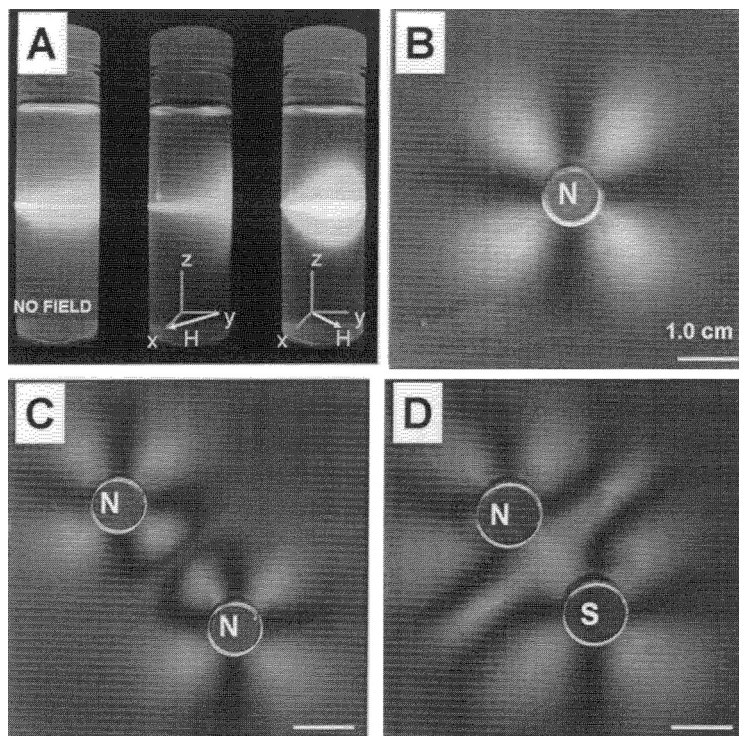


Figure 6. A) Anisotropic Mie scattering effects of magnetically aligned suspensions of plate-shaped NPCs **2** in ethanol. B-C) Birefringence patterns of a suspension of **2** in pyridine between two crossed polarizers and under the influence of a 6000 Oe magnetic field caused by one or two FeNdB magnets in front of the sample (north and south poles are marked as N and S). Reprinted in part with permission from refs. 28 and 31. Copyright 2002 and 2005 American Chemical Society.

the “hard” out-of-plane axis does assume no specific orientation. The lacking ability to control the hard magnetic axis of **2** puts a limit on the 3D controllability of these structures with a magnetic field. In terms of their magnetic orientation the plates behave analogously to magnetic rods (1).

As a result of their structural anisotropy, magnetically aligned dispersions of plate-shaped clusters **2** also acquire an optical anisotropy. Figure 7A shows a sample penetrated by laser light (532 nm) horizontally from the left. Depending on the orientations of the magnetic field lines (shown as arrow), the sample scatters maximum (100%) or minimum

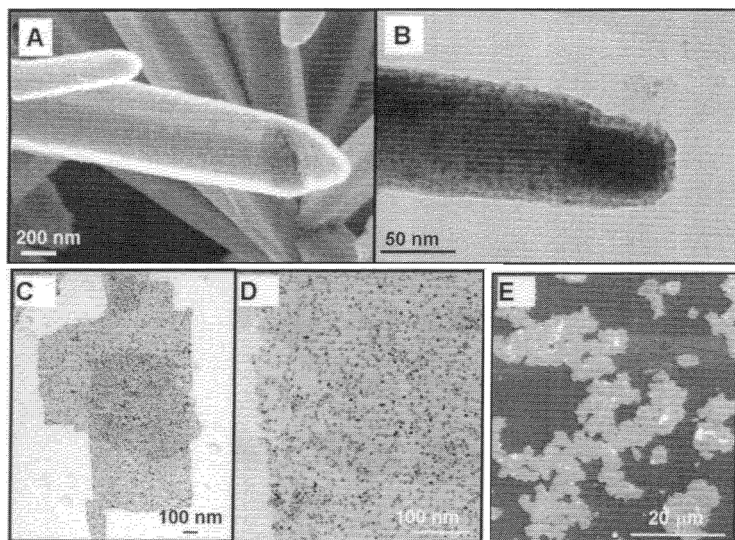


Figure 7. Micrographs of rod-shaped **4** and plate shaped **3**. ZnO-CdSe: A) SEM, B) TEM. $\text{Ca}_2\text{Nb}_3\text{O}_{10}$ -CdSe: C) TEM, D) increased magnification, E) SEM. Reprinted in part with permission from Refs. 32 and 34. Copyright 2005 American Chemical Society.

(30%) light intensity in the direction of the viewer. In this geometry, the plate-shaped NPCs behave as magnetic mirrors.

The birefringence patterns shown in Figures 7B-C arise when a sample of **2** in pyridine is placed between two cross-oriented polarizing filters and a magnetic field (6000 Oe) is turned on. Light areas in the patterns correspond to regions where the plate-shaped clusters are aligned so that they form 45° degree angles with the polarization directions of both polarization filters. The cluster alignment causes the polarization plane of the light to change so that it can pass the second polarization filter. In this experiment, the dispersion of **2** behaves similar to a liquid crystal.

2. LUMINESCENT NANOPARTICLE CLUSTERS

A key property of luminescent nanoparticles is that their emission wavelength can be adjusted with the particle size. As we will show here, the *direction* and *polarization* of the emission of CdSe nanoparticles can be controlled by assembling luminescent CdSe particles into rod-shaped and plate-shaped NPCs. The ability to modify the directional emission properties of semiconductor nanoparticles is of interest for applications

as optical probes,^[50] as components in photochemical cells,^[51] polarized light emitting devices,^[52] and lasers.^[24,35,53]

Planar clusters (3) of trioctylphosphineoxide (TOPO)-stabilized CdSe/CdS core/shell nanoparticles were synthesized following a protocol similar to that employed for superparamagnetic clusters 2 (Figure 2B) using amine-terminated $\text{Ca}_2\text{Nb}_3\text{O}_{10}$ nanoplates.^[34] Here the primary amine groups displace the weakly bonded TOPO from the CdSe nanoparticle surface establishing a covalent linkage. The reaction works with CdSe nanoparticles of sizes between 2 and 6 nm.

Rod-shaped CdSe containing clusters (4) were obtained by using ZnO microrods as structural templates.^[32] ZnO was chosen as a structural and optical support because of its high refractive index of 2.01, and because as a wide band gap semiconductor (3.2 eV) it does not absorb visible light. Reaction of the ZnO microrods with 3-aminopropyltrimethoxysilane (APS, Figure 2C) produced APS-terminated ZnO rods which, in a subsequent reaction with the CdSe nanoparticles in THF, underwent coupling to yield ZnO-CdSe clusters.

SEM and TEM micrographs (Figure 7AB) show that clusters 4 contain ZnO microrods that are coated with a dense 10 nm thick monolayer of CdSe particles. The sizes of the clusters ($6.85 \pm 1.73 \mu\text{m}$ long and $0.79 \pm 0.13 \mu\text{m}$ wide) are mainly determined by the sizes of the ZnO rods, which can be controlled by the conditions of ZnO synthesis.

The morphology of the plate-like NPCs 3 (Figure 7C-E) resembles that of clusters 2, except that Fe_3O_4 is replaced with CdSe. Both sides of the nanoplates are coated with particles at a density of 5340 ± 310 particles per square micrometer. Again, stacking occurs to produce multi-layer clusters with a mean length/width of $3.92 \pm 1.18 \mu\text{m}$ and with a thicknesses of $91 \pm 37 \text{ nm}$.

After excitation with light $< 550 \text{ nm}$, clusters 3 and 4 strongly emit in the visible. Figure 8A shows spectra for 4 emitting at yellow/green (563 nm), orange (593 nm), and red (617 nm), depending on the size of the CdSe nanocrystals (2.1–4.0 nm). In addition, the fluorescence spectra of rod-shaped 4 also contain an emission feature at 395 nm that corresponds to the band gap emission of ZnO. The CdSe emission quantum yield of the clusters is comparable to that of the free CdSe quantum dots in chloroform.

Wide field fluorescence micrographs of rod-shaped clusters 4 emitting at 563 nm are presented in Figure 8B. All clusters appear dark in the center and light at the end, which indicates that the emission occurs

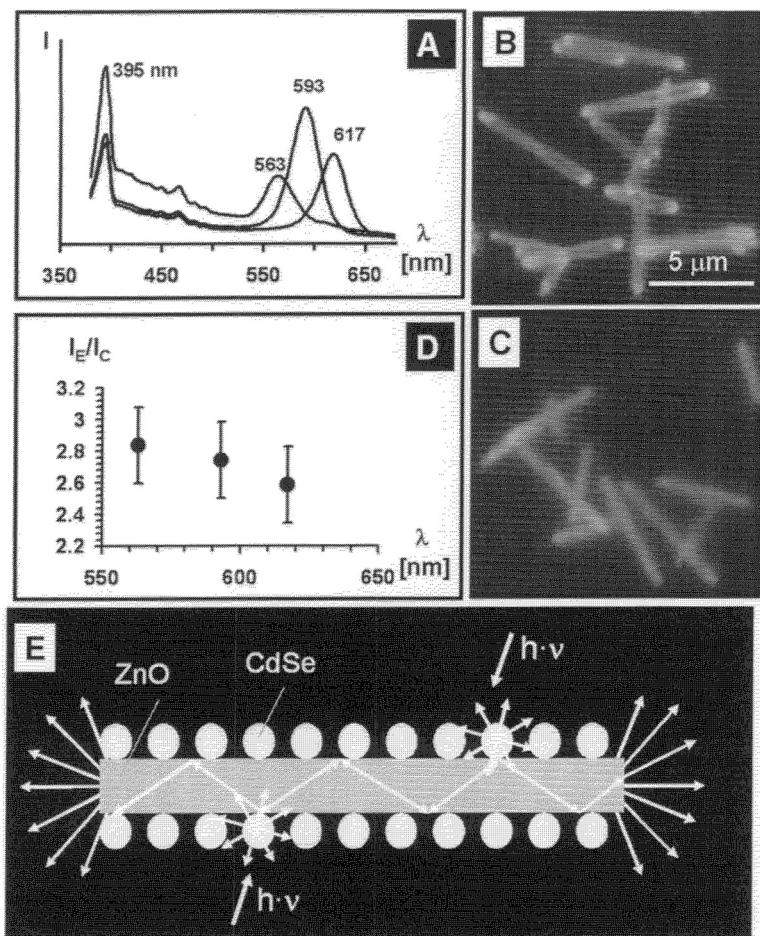


Figure 8. A) Fluorescence spectra of clusters 4 with three sizes of CdSe nanoparticles ($\lambda_{\text{ex}} = 300$ nm). Fluorescence micrographs of clusters under illumination with 330–380 nm light. B) on glass slide in air, C) on glass slide in oil ($n = 1.59$). Dependence of the directional emission ration on the emission wavelengths. E) schematic illustration of the waveguiding process in clusters 4. Reprinted in part with permission from Ref. 32. Copyright 2005 American Chemical Society.

predominantly at the rod ends. This effect is strongest for clusters that are not in direct contact with the Si substrate (i.e., for clusters that are supported by other clusters). On average the directional emission ratio I_E/I_C (with I_E and I_C as emission intensities of rod ends (I_E) and rod centers (I_C), respectively) is 2.72 ± 0.45 .

The directional emission observed in these structures is due to total internal reflection of light at the cluster air interface (Figure 8E). Light emitted by the quantum dots gets trapped inside the optically dense ZnO rods and migrates to the rod ends by total internal reflection at the ZnO-air interface. The effect vanishes when the clusters are immersed into an optically denser medium, such as a hydrocarbon oil (Figure 8C). Under these conditions, the optical interface between the clusters and the medium disappears. Because of scattering losses at the cluster air-interface, the directional emission on the clusters does not depend on the length or diameter of the structures. However, as Figure 8D shows, it weakly depends on the emission wavelengths (λ_{em}) of the microstructures. This indicates a transition from multimode ($W \gg 1$) to single mode ($W \ll 1$) waveguiding, which is expected from the waveguide parameter $W = (2\pi\delta/\lambda_{em})(n_{ZnO}^2 - n_{air}^2)$ for these structures, which lies between 3.49 and 3.67.^[54] In terms of their ability to guide light of variable wavelengths, the ZnO-CdSe clusters (4) thus represent the lower size limit.

Very similar directional emission effects can be observed in plate-like clusters 3 (Figure 9A). Here, the emitted light is most intense around the edges of individual clusters, whereas the centers remain relatively dark. The appearance of the micrographs changes when the clusters are tilted with respect to the viewing direction (Figure 9B). In these cases, the emission pattern take the shape of lines, which by SEM (supporting information of Ref.^[34]) can be shown to coincide with edges of the clusters. By placing a polarizing film between the sample and the eyepiece it can be established that the emission from the cluster edges is linearly polarized along the edges. This can be seen in Figure 9B, where the same sample region is shown for the indicated orientations of the polarizing film. The fact that the emission is polarized and enhanced with respect to the remainder of the film indicates that it arises from a waveguiding process inside the clusters. In contrast to cluster rods 4, the directional emission (expressed as I_R/I_C) of 3 strongly depends on the cluster thickness (Figure 9C). The smallest clusters that show the effect are about 70 nm thick, and thus contain ~ 4 layers of CdSe- $Ca_2Nb_3O_{10}$. Based on their thickness (70–160 nm), the cutoff wavelength for 3 should be 140–320 nm, i.e. light of greater wavelength should not be able to propagate in these structures. From this perspective, the observation of waveguided emission in <100 nm thick CdSe- $Ca_2Nb_3O_{10}$ clusters is unexpected. The enhanced waveguiding properties of these

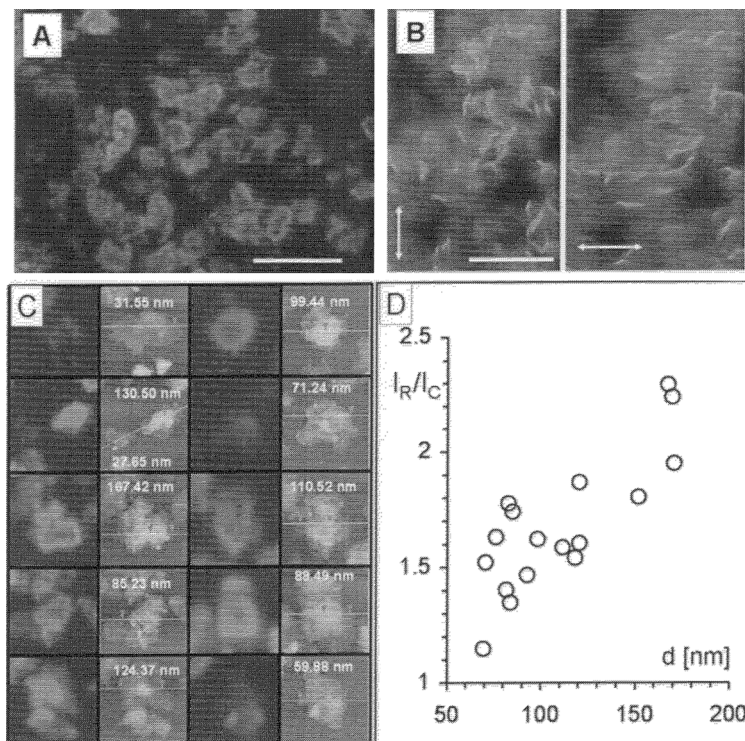


Figure 9. Optical micrographs (scale bar is 20 μm) of plate-shaped clusters 3 oriented parallel (A) or perpendicular (B) to the substrate. The arrows in B show the orientation of a polarizing film between the sample and the eyepiece. C) Optical micrographs and AFM topography scans on individual clusters 3. The measured cluster thicknesses are shown in the images. D) Plot of the directional emission ratio I_R/I_C (I_R = Intensity at the rim, I_C = Intensity in the center) against the measured thickness of the clusters. Reprinted in part with permission from Ref. 34. Copyright 2005 American Chemical Society.

structures are due to several factors. First, the refractive index (2.45) of the $\text{Ca}_2\text{Nb}_3\text{O}_{10}$ nanoplates is higher than for ZnO (2.01). Hence, one calculates 24° as the critical angle for total internal reflection at the cluster-air interface. Second, as molecular fragments of the Dion-Jacobsen phase $\text{KCa}_2\text{Nb}_3\text{O}_{10}$, exfoliated $\text{Ca}_2\text{Nb}_3\text{O}_{10}$ plates are atomically flat (see AFM scans in supporting material of Figure S-5 in reference).^[34] The small surface roughness of these plates minimizes scattering losses along the interface and maximizes reflection.

CONCLUSION

We have demonstrated that the optical emission and superparamagnetism of CdSe and Fe₃O₄ nanoparticles assume directional characteristics when these particles are incorporated into rod- or plate-shaped clusters. The orientations of the resulting uniaxial and biaxial superparamagnetic structures can be manipulated with weak magnetic fields. Plate-like clusters (2) behave like mirrors that turn in an applied magnetic field to reflect light into controllable directions. Such structures might be applicable as spatial waveguides or as magnetic valves. Uniaxial superparamagnetic clusters (1) can be used to stir microscale reaction mixtures, to drive microscale motors and actuators, or to transport drugs and spectroscopic probes into organisms. Uni- and bidirectional light emitters that emit polarized or non-polarized green, yellow, orange or red light upon irradiation with UV light could also be synthesized. The clusters could be of interest in light emitting devices with optimized contrast and polarization, or as optical probes that could provide spatial and orientational information about their environment. Our results suggest that the emission of other semiconductor nanocrystals can be similarly adjusted in three dimensions by combining them with microcrystals of other optically dense materials. The modular character of the *nanoparticle cluster assembly approach* thus presents an advantage over direct synthesis of emissive nanostructures, which is often limited to specific materials and conditions.

ACKNOWLEDGEMENTS

F. E. Osterloh thanks the National Science Foundation for support (CTS-0427418), Dr. S. Kauzlarich and Dr. B. Casey for equipment loans, and Dr. T. Guo for useful discussions.

REFERENCES

1. Zeng, H., J. Li, J. P. Liu, Z. L. Wang, and S. H. Sun, 2002. Exchange-coupled nanocomposite magnets by nanoparticle self-assembly. *Nature*, **420**(6914), 395–398.
2. Feldheim, D. L., K. C. Grabar, M. J. Natan, and T. E. Mallouk, 1996. Electron transfer in self-assembled inorganic polyelectrolyte/metal nanoparticle heterostructures. *J. Am. Chem. Soc.*, **118**(32), 7640–7641.
3. Musick, M. D., C. D. Keating, L. A. Lyon, S. L. Botsko, D. J. Pena, W. D. Holliway, T. M. McEvoy, J. N. Richardson, and M. J. Natan, 2000.

- Metal films prepared by stepwise assembly. 2. Construction and characterization of colloidal Au and Ag multilayers. *Chem. Mater.*, **12**(10), 2869–2881.
4. Hao, E. C., B. Yang, J. H. Zhang, X. Zhang, J. Q. Sun, and S. C. Shen, 1998. Assembly of alternating TiO₂/CdS nanoparticle composite films. *J. Mater. Chem.*, **8**(6), 1327–1328.
 5. Poznyak, S. K., D. V. Talapin, and A. I. Kulak, 2001. Structural, optical, and photoelectrochemical properties of nanocrystalline TiO₂-In₂O₃ composite solids and films prepared by sol-gel method. *J. Phys. Chem. B*, **105**(21), 4816–4823.
 6. Redl, F. X., K. S. Cho, C. B. Murray, and S. O'Brien, 2003. Three-dimensional binary superlattices of magnetic nanocrystals and semiconductor quantum dots. *Nature*, **423**(6943), 968–971.
 7. Murray, C. B., C. R. Kagan, and M. G. Bawendi, 2000. Synthesis and characterization of monodisperse nanocrystals and close-packed nanocrystal assemblies. *Ann. Rev. Mater. Sci.*, **30**, 545–610.
 8. Cumberland, S. L., M. G. Berrettini, A. Javier, and G. F. Strouse, 2003. Synthesis and characterization of a 1:6 Au-CdSe nanocomposite. *Chem. Mater.*, **15**(5), 1047–1056.
 9. Brust, M., C. J. Kiely, D. Bethell, and D. J. Schiffrin, 1998. C-60 mediated aggregation of gold nanoparticles. *J. Am. Chem. Soc.*, **120**(47), 12367–12368.
 10. Haremza, J. M., M. A. Hahn, and T. D. Krauss, 2002. Attachment of single CdSe nanocrystals to individual single-walled carbon nanotubes. *Nano. Lett.*, **2**(11), 1253–1258.
 11. Kolny, J., A. Kornowski, and H. Weller, 2002. Self-organization of cadmium sulfide and gold nanoparticles by electrostatic interaction. *Nano. Lett.*, **2**(4), 361–364.
 12. Crisp, M. T. and N. A. Kotov, 2003. Preparation of nanoparticle coatings on surfaces of complex geometry. *Nano. Lett.*, **3**(2), 173–177.
 13. Galow, T. H., A. K. Boal, and V. M. Rotello, 2000. A “building block” approach to mixed-colloid systems through electrostatic self-organization. *Adv. Mater.*, **12**(18), 576–579.
 14. Salgueirino-Maceira, V., F. Caruso, and L. M. Liz-Marzan, 2003. Coated colloids with tailored optical properties. *J. Phys. Chem. B*, **107**(40), 10990–10994.
 15. Caruso, F., M. Spasova, V. Saigueirino-Maceira, and L. M. Liz-Marzan, 2001. Multilayer assemblies of silica-encapsulated gold nanoparticles on decomposable colloid templates. *Adv. Mater.*, **13**(14), 1090–1094.
 16. Dong, A. G., Y. J. Wang, Y. Tang, N. Ren, W. L. Yang, and Z. Gao, 2002. Fabrication of compact silver nanoshells on polystyrene spheres through electrostatic attraction. *Chem. Commun.*, **4**, 350–351.

17. Fullam, S., H. Rensmo, S. N. Rao, and D. Fitzmaurice, 2002. Noncovalent self-assembly of silver and gold nanocrystal aggregates in solution. *Chem. Mater.*, **14**(9), 3643–3650.
18. Gomez, S., L. Erades, K. Philippot, B. Chaudret, V. Colliere, O. Balmes, and J. O. Bovin, 2001. Platinum colloids stabilized by bifunctional ligands: self-organization and connection to gold. *Chem. Commun.*, **16**, 1474–1475.
19. Shenton, W., S. A. Davis, and S. Mann, 1999. Directed self-assembly of nanoparticles into macroscopic materials using antibody-antigen recognition. *Adv. Mater.*, **11**(6), 449–452, 427.
20. Sapp, S. A., D. T. Mitchell, and C. R. Martin, 1999. Using template-synthesized micro- and nanowires as building blocks for self-assembly of supramolecular architectures. *Chem. Mater.*, **11**(5), 1183–1185, 5A.
21. Loweth, C. J., W. B. Caldwell, X. G. Peng, A. P. Alivisatos, and P. G. Schultz, 1999. DNA-based assembly of gold nanocrystals. *Angew. Chem., Int. Ed. Engl.*, **38**(12), 1808–1812.
22. Mirkin, C. A. 2000. Programming the assembly of two- and three-dimensional architectures with DNA and nanoscale inorganic building blocks. *Inorg. Chem.*, **39**(11), 2258–2272.
23. Sun, S. H., C. B. Murray, D. Weller, L. Folks, and A. Moser, 2000. Monodisperse FePt nanoparticles and ferromagnetic FePt nanocrystal superlattices. *Science*, **287**(5460), 1989–1992.
24. Klimov, V. I., A. A. Mikhailovsky, S. Xu, A. Malko, J. A. Hollingsworth, C. A. Leatherdale, H. J. Eisler, and M. G. Bawendi, 2000. Optical gain and stimulated emission in nanocrystal quantum dots. *Science*, **290**(5490), 314–317.
25. Kim, S. H., G. Medeiros-Ribeiro, D. A. A. Ohlberg, R. S. Williams, and J. R. Heath, 1999. Individual and collective electronic properties of Ag nanocrystals. *J. Phys. Chem. B*, **103**(47), 10341–10347.
26. Westcott, S. L., S. J. Oldenburg, T. R. Lee, and N. J. Halas, 1999. Construction of simple gold nanoparticle aggregates with controlled plasmon-plasmon interactions. *Chemical Physics Letters*, **300**(5–6), 651–655.
27. Westcott, S. L., S. J. Oldenburg, T. R. Lee, and N. J. Halas, 1998. Formation and adsorption of clusters of gold nanoparticles onto functionalized silica nanoparticle surfaces. *Langmuir*, **14**(19), 5396–5401.
28. Osterloh, F. E. 2002. Solution self-assembly of magnetic light modulators from exfoliated perovskite and magnetite nanoparticles. *J. Am. Chem. Soc.*, **124**(22), 6248–6249.
29. Hiramatsu, H. and F. E. Osterloh, 2003. pH-controlled assembly and disassembly of electrostatically linked CdSe-SiO₂ and Au-SiO₂ nanoparticle clusters. *Langmuir*, **19**(17), 7003–7011.
30. Osterloh, F., H. Hiramatsu, R. Porter, and T. Guo, 2004. Alkanethiol-induced structural rearrangements in silica-gold core-shell-type nanoparticle

- clusters: An opportunity for chemical sensor engineering. *Langmuir*, **20**(13), 5553–5558.
31. Kim, J. Y., F. E. Osterloh, H. Hiramatsu, R. K. Dumas, and K. Liu, 2005. Synthesis and real-time magnetic manipulation of a biaxial superparamagnetic colloid. *J. Phys. Chem. B*, **109**(22), 11151–11157.
 32. Kim, J. Y. and F. E. Osterloh, 2005. ZnO-CdSe nanoparticle clusters as directional photoemitters with tunable wavelength. *J. Am. Chem. Soc.*, **127**(29), 10152–10153.
 33. Osterloh, F. E., H. Hiramatsu, R. K. Dumas, and K. Liu, 2005. Fe₃O₄-LiMo₃Se₃ nanoparticle clusters as superparamagnetic nanocompasses. *Langmuir*, **21**(21), 9709–9713.
 34. Kim, J. Y., H. Hiramatsu, and F. E. Osterloh, 2005. Planar polarized light emission from CdSe nanoparticle clusters. *J. Am. Chem. Soc.*, **127**(44), 15556–15561.
 35. Cha, J. N., M. H. Bartl, M. S. Wong, A. Popitsch, T. J. Deming, and G. D. Stucky, 2003. Microcavity lasing from block peptide hierarchically assembled quantum dot spherical resonators. *Nano. Lett.*, **3**(7), 907–911.
 36. Artemyev, M. V., U. Woggon, R. Wannemacher, H. Jaschinski, and W. Langbein, 2001. Light trapped in a photonic dot: Microspheres act as a cavity for quantum dot emission. *Nano. Lett.*, **1**(6), 309–314.
 37. Fan, X. D., M. C. Lonergan, Y. Z. Zhang, and H. L. Wang, 2001. Enhanced spontaneous emission from semiconductor nanocrystals embedded in whispering gallery optical microcavities. *Phys. Rev. B*, **64**(11), 115310–115314.
 38. Shopova, S. I., G. Farca, A. T. Rosenberger, W. M. S. Wickramanayake, and N. A. Kotov, 2004. Microsphere whispering-gallery-mode laser using HgTe quantum dots. *Appl. Phys. Lett.*, **85**(25), 6101–6103.
 39. Nie, S. M. and S. R. Emery, 1997. Probing single molecules and single nanoparticles by surface-enhanced Raman scattering. *Science*, **275**(5303), 1102–1106.
 40. Chen, M. S. and D. W. Goodman, 2004. The structure of catalytically active gold on titania. *Science*, **306**(5694), 252–255.
 41. Zahn, M., 2001. Magnetic fluid and nanoparticle applications to nanotechnology. *Nanopart. Res.*, **3**(1), 73–78.
 42. Paxton, W. F., K. C. Kistler, C. C. Olmeda, A. Sen, S. K. St. Angelo, Y. Cao, T. E. Mallouk, P. E. Lammert, and V. H. Crespi, 2004. Catalytic nanomotors: autonomous movement of striped nanorods. *J. Am. Chem. Soc.*, **126**, 13426–13431.
 43. Tabiryan, N. V. and S. R. Nersisyan, 2004. Large-angle beam steering using all-optical liquid crystal spatial light modulators. *Appl. Phys. Lett.*, **84**(25), 5145–5147.
 44. Sayyah, K., C.-S. Wu, S.-T. Wu, and U. Efron, 1992. Anomalous liquid crystal undershoot effect resulting in a nematic liquid crystal-ased spatial light

- modulator with one millisecond response time. *Appl. Phys. Lett.*, **61**(8), 883–885.
45. Craighead, H. G. 2000. Nanoelectromechanical systems [Review]. *Science*, **290**(5496), 1532–1535.
 46. Tarascon, J. M., F. J. DiSalvo, C. H. Chen, P. J. Carroll, M. Walsh, and L. Rupp, 1984. First example of monodispersed (Mo₃Se₃) clusters. *J. Solid State Chem.*, **58**, 290–300.
 47. Tarascon, J. M., G. W. Hull, and F. J. DiSalvo, 1984. A facile synthesis of Pseudo one-dimensional ternary molybdenum chalcogenides M₂Mo₆X₆ (X = Se, Te; M = Li, Na, Cs). *Mater. Res. Bull.*, **19**, 915–924.
 48. Sun, S. H. and H. Zeng, 2002. Size-controlled synthesis of magnetite nanoparticles. *J. Am. Chem. Soc.* **124**(28), 8204–8205.
 49. Schaak, R. E. and T. E. Mallouk, 2000. Self-assembly of tiled perovskite monolayer and multiplayer thin films. *Chem. Mater.*, **12**(9), 2513–2516.
 50. Bruchez, M., M. Moronne, P. Gin, S. Weiss, and A. P. Alivisatos, 1998. Semiconductor nanocrystals as fluorescent biological labels. *Science*, **281**(5385), 2013–2016.
 51. Huynh, W. U., X. Peng, and A. P. Alivisatos, 1999. CdSe nanocrystal rods/poly(3-hexylthiophene) composite photovoltaic devices. *Adv. Mat.*, **11**(11), 923–927.
 52. Hikmet, R. A. M., P. T. K. Chin, and T. P. Talapin, 2005. Polarized-light-emitting quantum-rod diodes. *Adv. Mater.*, **17**, 1436–1439.
 53. Eisler, H. J., V. C. Sundar, M. G. Bawendi, M. Walsh, H. I. Smith, and V. Klimov, 2002. Color-selective semiconductor nanocrystal laser. *Appl. Phys. Lett.*, **80**(24), 4614–4616.
 54. Snyder, A. W. and J. D. Love, 1983. Optical Waveguide Theory. Chapman and Hall, New York, p. viii, 734.